Pergamon

Int. J. Heat Mass Transfer. Vol. 37, No. 3, pp. 469–478, 1994

0017-9310/94 $6.00+0.00

Parametric study of turbulent three-dimensional heat transfer of arrays of heated blocks encountered in electronic equipment

Y. ASAKO
Department of Mechanical Engineering, Tokyo Metropolitan University, Tokyo 192-03, Japan

and

MOHAMMAD FAGHRI
Department of Mechanical Engineering, University of Rhode Island, Kingston, RI 02881, U.S.A.

(*Received* 31 *August* 1992 *and in final form* 28 *June* 1993)

Abstract—Periodic fully developed fluid flow and heat transfer characteristics are obtained numerically for turbulent flow over three-dimensional arrays of heated square blocks deployed along one wall of a parallel-plate duct. This configuration simulates forced convection cooling of electronic equipment. The high Reynolds number form of the k–ε turbulence model is used for the computations. The computations are performed for the condition of uniform wall temperature, for a wide range of geometric parameters characterizing the array, for a range of Reynolds numbers from 10^4 to 10^5, and for Prandtl number of 0.7. The results show that the friction factor is higher or lower than the values obtained from an empirical correlation for a parallel-plate duct depending on the geometric parameters and the Reynolds number. The cycle averaged Nusselt number is also higher or lower than the analytical values for a parallel-plate duct with one wall heated at a constant rate and the other wall insulated depending on the geometric parameters and the Reynolds number.

INTRODUCTION

IN CURRENT electronic packaging designs of low power rated electronic components on printed circuit boards, specific consideration is given to heat transfer analysis to achieve high heat dissipation rates and to limit peak temperature levels (e.g. Oktay *et al.* [1]). This concern has generated motivation for research studies in the forced convection cooling of electronic equipment containing printed circuit boards. In most of the recent literature, an array of heated square blocks deployed along one wall of a parallel-plate duct is used to model the circuit board.

The authors (Asako and Faghri [2]) reported a three dimensional laminar heat transfer analysis of this problem under the condition where the blocks were at a prescribed uniform wall temperature. As an extension of this work, they (Asako and Faghri [3]) computed the results of this problem under a different thermal boundary condition. It was assumed that a specific amount of heat was uniformly generated at the bottom surface of each block. These analyses were performed for the periodic fully developed region with the assumption of laminar flow.

Experimental investigations of similar configurations were carried out by Sparrow *et al.* [4–6], and Moffat *et al.* [7]. However, these investigations were for a fixed or limited set of geometrical parameters. The authors (Faghri *et al.* [8]) reported experimental results for a wider range of geometric parameters.

As an extension of the analyses for laminar flow, the authors (Faghri and Asako [9]) reported the results for turbulent flow using the high Reynolds number form of the k–ε turbulence model. The average heat transfer coefficients and the friction factor were compared with the available experimental results. However, the computations were performed for a fixed set of geometrical parameters. The range of the Reynolds number of the computations did not coincide with that of the experiment and no direct comparisons could be made. However, the numerical results were located on an extended line of the experimental data. This is the motivation of the present work for a parametric study for a wider range of geometric parameters characterizing the array, for a range of Reynolds numbers from 10^4 to 10^5, and for a Prandtl number of 0.7. The turbulent model employed is the high Reynolds number form of the k–ε turbulence model. The results are obtained for the condition of uniform wall temperature and are compared with the available experimental and analytical results.

FORMULATION

Description of the problem

The problem to be considered in this study is depicted schematically in Fig. 1. It involves the determination of three-dimensional heat transfer and fluid flow characteristics for turbulent forced-convection cooling of an array of square heat generating modules.

NOMENCLATURE

A_H	flow cross section above modules
A_w	per-cycle heat transfer surface area
B	module thickness
C_p	specific heat of the fluid at constant pressure
f	friction factor, equation (9)
H	height of flow passage
h	local heat transfer coefficient, equation (11)
h_m	cycle averaged heat transfer coefficient, equation (12)
K	thermal conductivity
k	turbulence kinetic energy
L	plane dimension of square module
$\dot{m}$	mass flow rate per spanwise width
Nu	local Nusselt number, equation (15)
Num	cycle averaged Nusselt number, equation (16)
n	coordinate normal to the module
P	production term
p	pressure
p'	periodic component of pressure
p^*	redefined pressure
Q	heat
q	heat flux
Re	Reynolds number, equation (8)
S	intermodule gap
T	dimensionless temperature, equation (2)
t	temperature
t_b	bulk temperature, equation (3)
t_w	module surface temperature
u, v, w	velocity components
$\bar{w}$	characteristic velocity, equation (7)
x, y, z	coordinates.

Greek symbols

β	per-cycle pressure gradient
Γ	diffusion coefficient
γ	wall-to-bulk temperature ratio
ε	turbulence dissipation rate
Λ	periodic parameter defined in Table 1
λ	periodic parameter defined in Table 1
μ	viscosity
μ_t	turbulent viscosity
ν	kinematic viscosity
ρ	density
σ	Prandtl number
ϕ	dependent variables.

The modules are positioned along one wall of a thermally insulated parallel-plate duct. The geometry of the problem is specified by the module dimension (L), the module thickness (B), the inter-module gap (S), and the height of the flow passage between the module and the opposite wall of the duct (H).

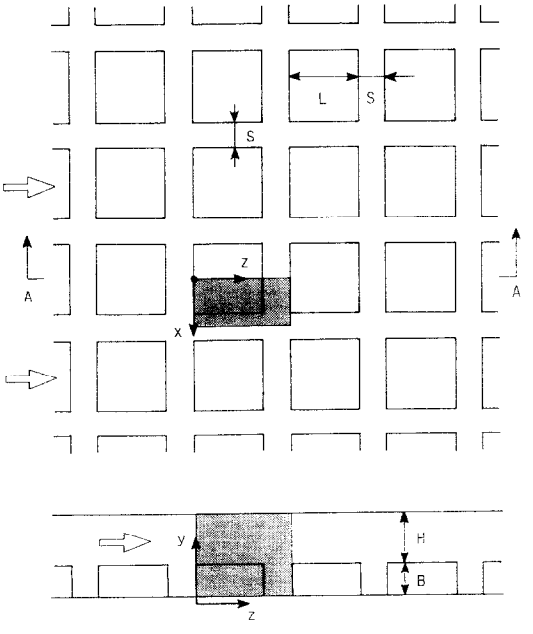

FIG. 1. Schematic diagram of array of rectangular modules deployed along one wall of a flat parallel plates duct.

The solution domain, with the assumption of periodic fully developed flow, is confined to a typical module shaded in Fig. 1. As described by Pantankar *et al.* [10], the periodic fully developed flow is characterized by a velocity field that repeats itself at corresponding axial stations in successive cycles. Furthermore, in such a regime, the pressures of cyclically corresponding locations decrease linearly in the downstream direction. The pressure, p, is expressed by

$$p(x, y, z) = -\beta z + p'(x, y, z) \quad (1)$$

where β is a constant, and $p'(x, y, z)$ behaves in a periodic manner from module to module. The term βz represents the non-periodic pressure drop that takes place in the flow direction.

For the case of uniform wall temperature boundary condition, the fluid temperature approaches the wall temperature in the fully developed region. Therefore, the following dimensionless temperature will be introduced,

$$T(x, y, z) = [t(x, y, z) - t_w]/(t_b - t_w) \quad (2)$$

where

$$t_b - t_w = \int\int (t - t_w) w \, dx \, dy \Big/ \int\int w \, dx \, dy. \quad (3)$$

For the periodic thermally developed region, the dimensionless temperature satisfies the following relationship:

$$T(x, y, z) = T(x, y, z + L + S) = T(x, y, Z + 2L + 2S) = \cdots. \quad (4)$$

Table 1. Summary of equations solved

Equation	ϕ	Γ	S_ϕ
Continuity	1	0	0
x momentum	u	μ_{eff}	$\partial\{\mu_{eff}(\partial u/\partial x)\}/\partial x+\partial\{\mu_{eff}(\partial v/\partial x)\}/\partial y+\partial\{\mu_{eff}(\partial w/\partial x)\}/\partial z-\partial p^*/\partial x$
y momentum	v	μ_{eff}	$\partial\{\mu_{eff}(\partial u/\partial y)\}/\partial x+\partial\{\mu_{eff}(\partial v/\partial y)\}/\partial y+\partial\{\mu_{eff}(\partial w/\partial y)\}/\partial z-\partial p^*/\partial y$
w momentum	w	μ_{eff}	$\partial\{\mu_{eff}(\partial u/\partial z)\}/\partial x+\partial\{\mu_{eff}(\partial v/\partial z)\}/\partial y+\partial\{\mu_{eff}(\partial w/\partial z)\}/\partial z-\partial p^*/\partial z+\beta$

where

$$p^* = p' + (2/3)k\rho$$

Energy	T	$\mu/\sigma+\mu_t/\sigma_t$	Λ
Turbulence energy	k	$\mu+\mu_t/\sigma_k$	$P-\rho\varepsilon$
Energy dissipation	ε	$\mu+\mu_t/\sigma_\varepsilon$	$(C_1P-C_2\rho\varepsilon)\varepsilon/k$

where

$$\mu_{eff} = \mu+\mu_t$$
$$\mu_t = C_\mu\rho k^2/\varepsilon$$
$$P = \mu_t[2\{(\partial u/\partial x)^2+(\partial v/\partial y)^2+(\partial w/\partial z)^2\}+(\partial u/\partial y+\partial v/\partial x)^2+(\partial w/\partial x+\partial u/\partial z)^2+(\partial v/\partial z+\partial w/\partial y)^2]$$
$$\Lambda = [\Gamma(\partial T/\partial z)+\partial(\Gamma T)/\partial z-\rho wT]\lambda+\Gamma T(\lambda^2+\mathrm{d}\lambda/\mathrm{d}z)$$

and

$$\lambda = [\partial(t_b-t_w)/\partial z]/(t_b-t_w)$$

and constants are

$$C_\mu = 0.09,\ C_1 = 1.44,\ C_2 = 1.92,\ \sigma_k = 1.0,\ \sigma_\varepsilon = 1.3 \text{ and } \sigma_t = 0.9$$

Therefore, the fully developed dimensionless temperature field repeats itself at corresponding axial stations in successive cycles.

Conservation equations

The governing equations to be considered are the time-averaged continuity, momentum, and energy equations. An eddy viscosity model is used to account for the effect of turbulence. The model chosen is the high Reynolds number form of the k–ε (turbulence kinetic energy–turbulence dissipation rate) model. Constant thermophysical properties are assumed, and natural convection is excluded. The $(2/3)k\rho$ term is absorbed in the pressure gradient by redefining the pressure p^*. Then, the governing equations can be written in the common form as:

$$\partial(\rho u\phi)/\partial x+\partial(\rho v\phi)/\partial y+\partial(\rho w\phi)/\partial z = S_\phi+\partial\{\Gamma_{eff}(\partial\phi/\partial x)\}/\partial x+\partial\{\Gamma_{eff}(\partial\phi/\partial y)\}/\partial y+\partial\{\Gamma_{eff}(\partial\phi/\partial z)\}/\partial z \quad (5)$$

where ϕ stands for different dependent variables (u, v, w, T, k, and ε). The equations used in this paper are summarized in Table 1. The terms Λ and λ are periodic parameters arising from the assumption of constant wall temperature boundary condition. These values are determined as a part of the solution process.

To complete the formulation of the problem, the boundary conditions remain to be discussed. These are

On the duct walls:

$$u = v = w = \partial T/\partial y = 0$$

On the module surfaces:

$$u = v = w = 0, \quad T = 0$$

On the symmetric planes:

$$u = \partial v/\partial x = \partial w/\partial x = \partial T/\partial x = 0. \quad (6)$$

As a preliminary study, the wall function treatment for the fully turbulent region proposed by Launder and Spalding [11] is employed. Namely, the universal velocity profile is used for the u, v, w equations. For the k equation, the diffusion flux to the wall is considered to be zero. For the ε equation, the value at the near-wall grid point is fixed. As an example, the wall function treatment for the top surface of the module is summarized in Table 2. The wall function treatment for the other surface is similar to one for the top surface. At the inlet and outlet ends of the solution domain, periodic conditions are imposed.

Table 2. Summary of wall function treatment

For w equation:

$$\Gamma_B = \mu y^+/w^+$$

where

$$y^+ < 11.5 : w^+ = y^+$$
$$y^+ > 11.5 : w^+ = 2.5\ln(9y^+)$$

and where

$$y^+ = \rho k^{1/2}C_\mu^{1/4}y/\mu$$

For k equation: $\Gamma_B = 0$

For ε equation: $\varepsilon = (C_\mu k^2)^{3/4}/(0.4y)$

For T equation,

$$y^+ < 11.5 : \Gamma_B = \mu/\sigma$$
$$y^+ > 11.5 : \Gamma_B = \mu y^+/\{\sigma_T[2.5\ln(9y^+)]+\Phi\}$$

where

$$\Phi = 9(\sigma/\sigma_T-1)(\sigma/\sigma_T)^{-1/4}$$

Namely, inlet conditions are set equal to outlet conditions for all the variables.

Numerical solution

The control volume approach is adopted to solve equation (5) by a finite difference scheme. The discretized procedure of the equations is based on the power law scheme of Patankar [12], and the discretized equations are solved by using a line-by-line method. Alternating sweeps of cyclic TDMA in the z direction and normal TDMA in the x and y directions are applied. The pressure and velocity are linked by the SIMPLE algorithm of Patankar [13]. The three-dimensional computer code used for this problem is a modified version of the two-dimensional computer code SIMPLE. Computations are performed with the same grid distribution ($16\times22\times30$) which was used in the previous work. These grid points are distributed in a non-uniform manner with higher concentration of grids closer to the walls. The grid independence test results were reported in the author's previous paper (Faghri and Asako [9]).

The values of β have to be specified prior to the initiation of the numerical solution. These values are selected such that the calculated Reynolds numbers range from 10^4 to 10^5. In some literature (e.g. Patankar and Prakash [14] and Lee *et al.* [15]) dealing with the periodic fully developed problems, the Reynolds number is also specified. In this case, the viscosity or the value of β is adjusted to obtain the solution for a given Reynolds number. However, in the present investigation, the Reynolds number is not specified prior to the initiation of the numerical solution.

The convergence criterion used in this computation was that the value of the mass flux residuals (mass flow) in each control volume took a value under 10^{-10}. The under-relaxation factors for the velocity, the pressure, the turbulence kinetic energy, and the energy dissipation rate were set to 0.5, 0.8, 0.4, and 0.4, respectively. About 4000–14000 iterations were required to obtain a converged solution for the velocity field. The number of the iterations depended on the Reynolds number and geometric parameters. The converged velocity field was used as an input to the temperature field calculation, which converged to within 300 iterations.

Reynolds number, pressure drop, and Nusselt number

Attention will now be focused on the calculation of the Reynolds number. Since the gap height H between the modules and the opposite wall of the duct is regarded as the main passage for fluid flow, a characteristic velocity is evaluated from

$$\rho\bar{w} = \dot{m}/A_H \tag{7}$$

in which A_H is the flow cross section associated with the gap height H and $\dot{m}$ is the mass flow rate per span-wise width. Consistent with the foregoing, H will be selected as the characteristic dimension in the Reynolds number to obtain

$$Re = \rho\bar{w}H/\mu = \dot{m}/[\mu(A_H/H)] \tag{8}$$

where the quantity (A_H/H) is the span-wise width of the flow passage.

Another quantity is the calculation of pressure drop. It is of practical interest to compare this quantity with the corresponding value obtained for the straight duct. The friction factor f is defined as

$$f = \beta(2H)/[(\rho\bar{w}^2)/2]. \tag{9}$$

Since the Reynolds number is based on H, the friction factor by this definition for laminar Hagen–Poiseuille flow can be expressed as

$$f = 48/Re. \tag{10}$$

The local heat transfer coefficient h and cycle average heat transfer coefficient h_m will be defined as

$$h = q/(t_w - t_b) \tag{11}$$

$$h_m = Q/A_w(\overline{t_w - t_b}) \tag{12}$$

where q is the local heat flux, A_w is the per-cycle transfer surface area, equal to L^2+4BL, Q is the heat transfer rate from the module to the fluid per cycle, and $(\overline{t_w - t_b})$ is the average wall-to-bulk temperature difference. The log mean temperature difference is expressed by

$$\overline{t_w - t_b} = (t_w - t_b)_{z=0}(1-\gamma)\Big/\left(-\int_0^{L+S}\lambda\,dz\right) \tag{13}$$

where

$$\gamma = \exp\left[\int_0^{L+S}\lambda\,dz\right]. \tag{14}$$

The Nusselt number expressions obtained by assuming log mean temperature difference with the wall function treatment are as follows:

$$\begin{aligned} Nu &= h(2H)/K = -2H(\partial t/\partial n)_w/(t_w - t_b) \\ &= 2H\{\Gamma_B/(\mu/\sigma)\}(T_1/n_1) \end{aligned} \tag{15}$$

$$\begin{aligned} Nu_m &= h_m(2H)/K \\ &= 2H\left(-\int_0^{L+S}\lambda\,dz\right)\left[C_p\dot{m}/K - \int\{\lambda T - \partial T/\partial z\}_{z=0}\,dx\,dy\right]\Big/A_w \\ &= 2H\left(-\int_0^{L+S}\lambda\,dz\right)\left[Re\,\sigma(L+S) - \int\{\lambda T - \partial T/\partial z\}_{z=0}\,dx\,dy\right]\Big/A_w \end{aligned} \tag{16}$$

where n is the coordinate normal to the heated surface, K is the thermal conductivity, and the suffix I indicates the first internal grid point near the wall.

RESULTS AND DISCUSSION

The geometry of the problem is specified by the module dimension (L), the module thickness (B), the inter-module gap (S), and the height of the flow passage between the module and the opposite wall of the duct (H). If L is chosen as a characteristic length, then the dimensionless geometric parameters in the problem are B/L, S/L, and H/L. The computations are performed for $B/L = 3/8$ and $1/2$, and for $S/L = 1/2$, $1/3$, $1/4$, and $1/5$. The values of $5/8$, $3/8$, and $1/4$ are selected for H/L for the case of $B/L = 3/8$ and $3/4$, $1/2$, and $1/4$ are selected for H/L for $B/L = 1/2$. In this paper, a value of 0.7 is used for the Prandtl number, σ, and the values chosen for β are selected such that the calculated Reynolds numbers range from 10^4 to 10^5.

Velocity profile

The locations of the vertical planes at $z = 0$, $L/2$, L, and $L+S/2$ are shown speckled in Fig. 2. The representative profiles of the velocity component w for $B/L = 1/2$, $S/L = 1/3$ and $H/L = 1/4$ at these planes for $Re = 2.91 \times 10^4$ are presented in Figs. 3(a)–(d). As seen from these figures, the magnitude of the w velocity component in the inter-module gap in the stream-wise direction is slightly faster than that over the module. Comparing Figs. 3(a)–(d), it can be seen that the velocity profiles at each plane are almost the same with the exception of the profile in Fig. 3(d). In this profile a very weak reverse flow can be seen in the inter-module gap in the span-wise direction. It is noteworthy that the velocity profile for the turbulent flow is flat compared with that for the laminar flow.

From the characteristics of the velocity profiles, it can be easily predicted that the fluid flow in the inter-module gap in the stream-wise direction plays a role of decreasing the friction factor. However, the existence of the inter-module gap in the span-wise direction will increase the turbulence and it results in an increase of the friction factor. Similar characteristics for a two-dimensional problem were reported in the literature by Knight and Crawford [16].

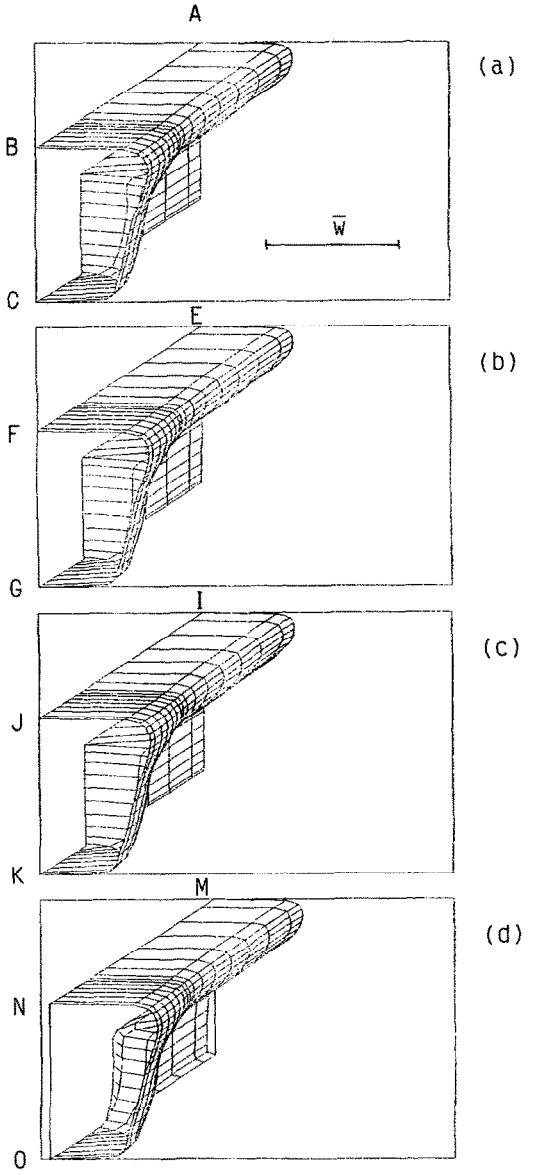

FIG. 3. Velocity profiles at vertical planes for $B/L = 1/2$, $S/L = 1/3$, $H/L = 1/4$ and $Re = 2.91 \times 10^4$: (a) $z = 0$, (b) $z = L/2$, (c) $z = L$, and (d) $z = L+S/2$.

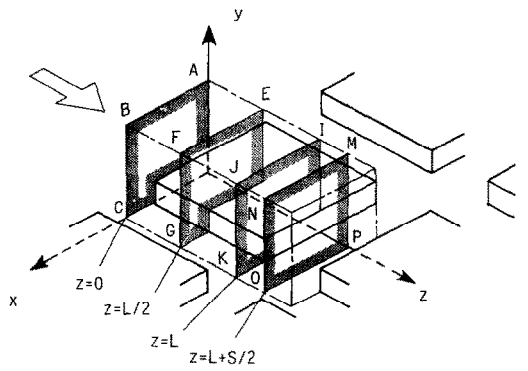

FIG. 2. Schematic view of the location of planes in Fig. 3.

Friction factor

The friction factor, f, for $B/L = 3/8$, $S/L = 1/4$ and $H/L = 5/8$ is compared with the experimental data obtained by Sparrow *et al.* [4] in Fig. 4. A good agreement between experimental and numerical friction factors can be seen. The empirically obtained correlation of Beavers *et al.* [17] for the turbulent flow in a parallel-plate duct is also plotted in the figure. The friction factor for the Hagen–Poiseuille laminar flow of a duct of height H is also plotted in this figure. The Reynolds number is based on the duct height, H, so that the friction factor for the Hagen–Poiseuille flow can be expressed by $f = 48/Re$. Since the friction

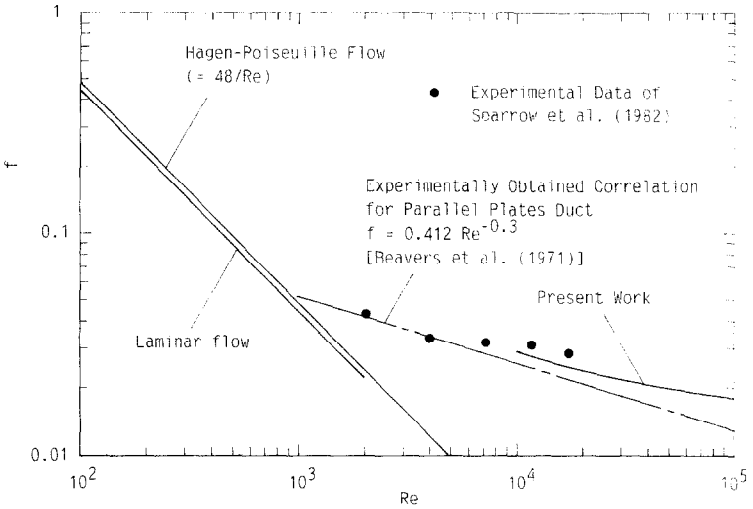

FIG. 4. Comparison of friction factors with previous data for $B/L = 3/8$, $S/L = 1/4$, and $H/L = 5/8$.

factor is based on the characteristic velocity, w, it is lower than the values for the parallel-plate duct in the laminar region because of the existence of the flow in the inter-module gap in the streamwise direction. However, in the turbulent region, the inter-module gap generates turbulence and it results in an increase of the friction factor. In this case, the friction factor is higher than that for the parallel-plate duct.

The results for the friction factors for $B/L = 3/8$ and 1/2 are plotted in Figs. 5 and 6 as a function of

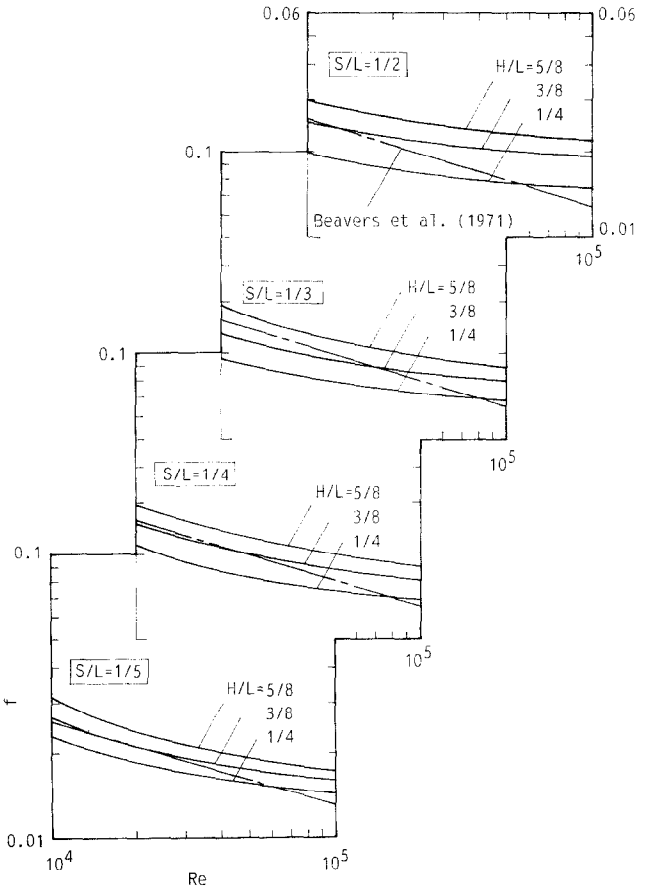

FIG. 5. Friction factor, f, as a function of Reynolds number for $B/L = 3/8$.

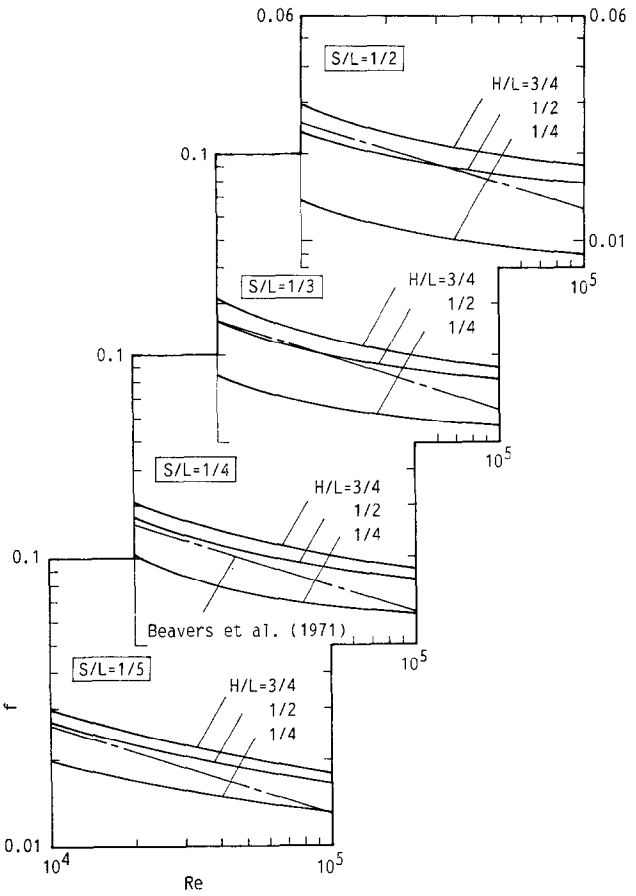

FIG. 6. Friction factor, f, as a function of Reynolds number for $B/L = 1/2$.

Reynolds number with the height of the flow passage as a curve parameter. The empirically obtained correlations of Beavers *et al.* [17] for turbulent flow in a parallel-plate duct is also plotted in the figures. As expected, the friction factor is higher or lower than that for the parallel-plate duct depending on the geometric parameters and the Reynolds number. The friction factor decreases with a decrease in the height of the flow passage because of the existence of the flow in the inter-module gap in the stream-wise direction. This tendency is accentuated in a case of a wide inter-module gap ($S/L = 1/2$) and a thick module ($B/L = 1/2$). As seen from the figure, the friction factor decreases with the Reynolds number. However, it has a weak dependency on the Reynolds number compared with the correlation for parallel-plate duct.

Local Nusselt number

The local Nusselt number on each surface of the rectangular module for $B/L = 1/2$, $S/L = 1/3$, $H/L = 1/4$, and $Re = 2.91 \times 10^4$ is shown in Fig. 7. In this figure, the local Nusselt number on the top surface, the front surface, the side surface, and the rear surface of the module is shown in parts (a)–(d), respectively. The corners are marked with letters such as A, B, ... in a module in Fig. 8. As seen from the figure, the Nusselt number values at the corners A and B are high. This tendency is similar to that for the laminar flow. The Nusselt number on the front and rear surfaces are lower. In other words, the front and rear surfaces do not contribute to the heat transfer from the module. This result can be easily expected, since the recirculation in the inter-module gap is very weak.

Cycle averaged Nusselt number

The cycle averaged Nusselt number, defined by equation (16), is plotted as a function of Reynolds number in Figs. 9–12 with the height of the flow passage as a curve parameter for a number of intermodule gap spacings. In the figures, an analytical result by Kays and Leung [18] for fully developed turbulent flow in a parallel-plate duct with one wall heated at a constant rate and the other wall insulated, is also plotted. Although the thermal boundary condition used for the analytical problem is different from the one used for the present numerical analysis, the Nusselt number is higher or lower than this analytical value depending on the geometric parameters and Reynolds number. The Nusselt number decreases with a decrease in the height of the flow passage. This tendency is slightly accentuated in the case of a wide

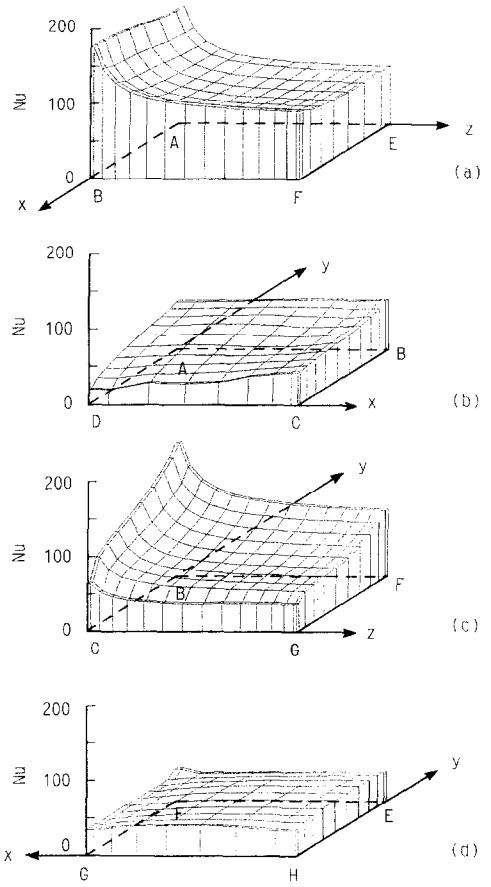

FIG. 7. Local Nusselt number for $B/L = 1/2$, $S/L = 1/3$, $H/L = 1/4$ and $Re = 2.91 \times 10^4$ on (a) top, (b) front, (c) side, and (d) rear surfaces (refer to Fig. 8 for letters at the corners).

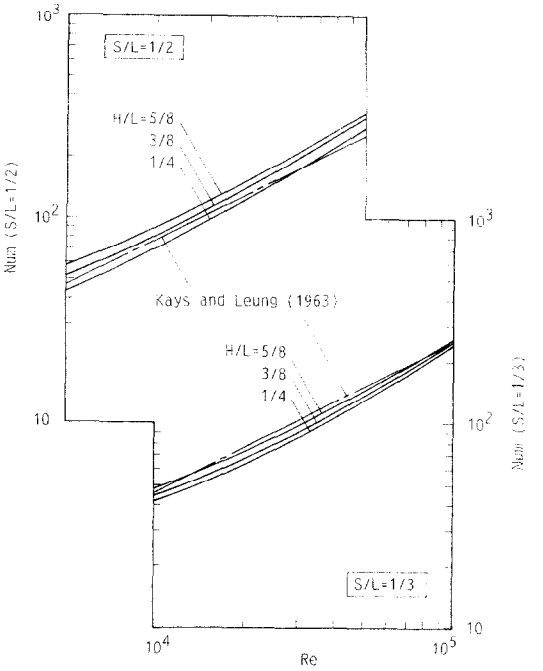

FIG. 9. Cycle-averaged Nusselt number, *Num*, as a function of Reynolds number for $B/L = 3/8$ ($S/L = 1/2$ and $1/3$).

intermodule gap ($S/L = 1/2$). It can be seen from the figures that the Nusselt number decreases with a decrease in the intermodule gap.

CONCLUDING REMARKS

Periodic fully developed fluid flow and heat transfer characteristics are obtained numerically for turbulent flow over three-dimensional arrays of heated square blocks deployed along one wall of a parallel plates duct. The computations were performed for a wide range of the geometric parameters characterizing the array and for a range of Reynolds numbers from 10^4 to 10^5, and for Prandtl number of 0.7. The main conclusions are as follows:

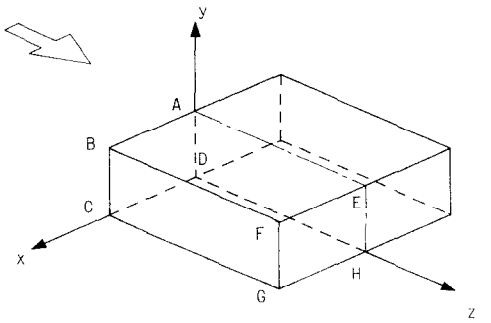

FIG. 8. Schematic view of a module and the nomenclature used in Fig. 7.

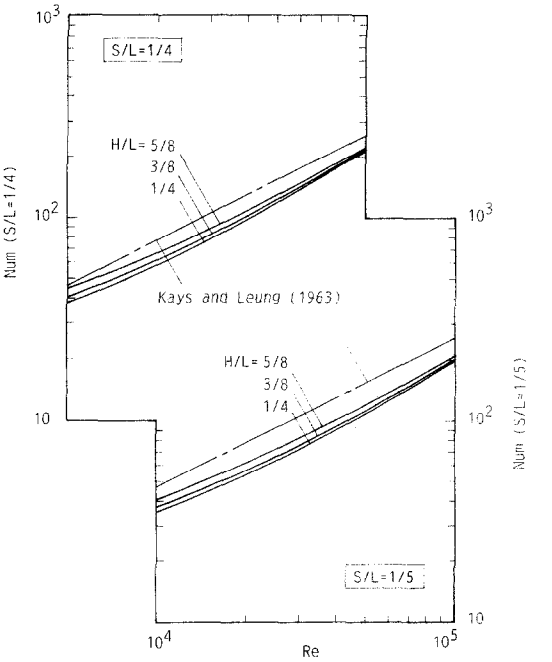

FIG. 10. Cycle-averaged Nusselt number, *Num*, as a function of Reynolds number for $B/L = 3/8$ ($S/L = 1/4$ and $1/5$).

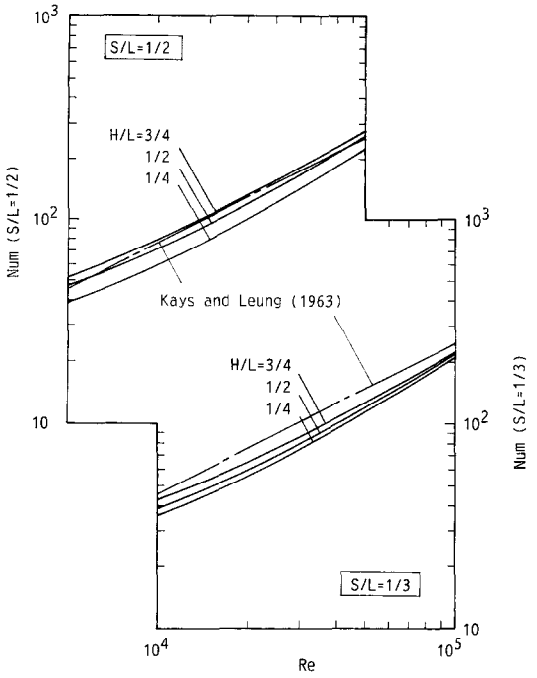

FIG. 11. Cycle-averaged Nusselt number, *Num*, as a function of Reynolds number for $B/L = 1/2$ ($S/L = 1/2$ and 1/3).

(a) The friction factor for arrays of rectangular modules agrees well with the available experimental values and it is higher or lower than that for the parallel-plate duct depending on the geometric parameters and the Reynolds number.

(b) The friction factor decreases with a decrease in the height of the flow passage because of the existence of the flow in the inter-module gap in the stream-wise direction. This tendency is accentuated in a case of a wide inter-module gap ($S/L = 1/2$) and a thick module ($B/L = 1/2$).

(c) The friction factor decreases with the Reynolds number. However, it has a weak dependency on the Reynolds number compared with the correlation for parallel-plate duct.

(d) The cycle averaged Nusselt number decreases with a decrease in the height of the flow passage. This tendency is slightly accentuated in the case of wide inter-module gap ($S/L = 1/2$).

(e) The cycle averaged Nusselt number decreases with a decrease in the intermodule gap.

(f) The cycle averaged Nusselt number is also higher or lower than the analytical value for the parallel-plate duct with one wall heated at a constant rate and the other wall insulated depending on the geometric parameters and the Reynolds number.

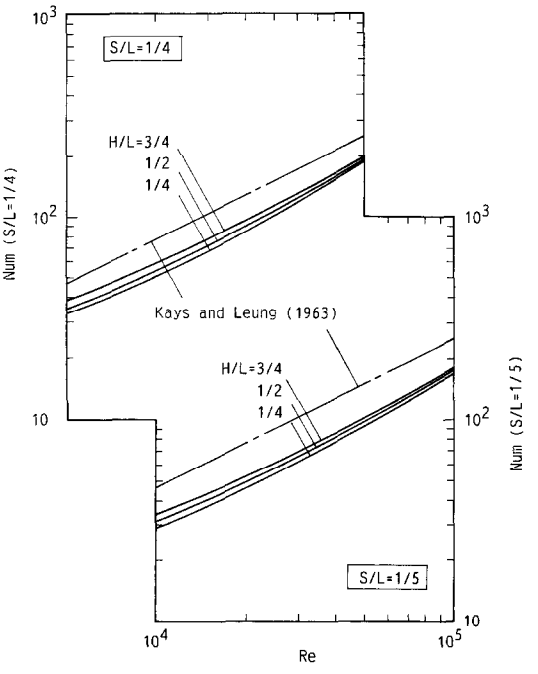

FIG. 12. Cycle-averaged Nusselt number, *Num*, as a function of Reynolds number for $B/L = 1/2$ ($S/L = 1/4$ and 1/5).

REFERENCES

1. C. Oktay, R. Hannemann and A. Bar-Cohen, High heat from a small package, *Mech. Engng* **108,** 36–42 (1986).
2. Y. Asako and M. Faghri, Three-dimensional heat transfer and fluid flow analysis of rectangular blocks encountered in electronic equipment, *Numer. Heat Transfer* **13,** 481–498 (1988).
3. Y. Asako and M. Faghri, Three-dimensional heat transfer analysis of arrays of heated square blocks, *Int. J. Heat Mass Transfer* **32,** 395–405 (1989).
4. E. M. Sparrow, J. E. Niethammaer and A. Chaboki, Heat transfer and pressure drop characteristics of arrays of rectangular modules encountered in electronic equipment, *Int. J. Heat Mass Transfer* **25,** 961–973 (1982).
5. E. M. Sparrow, S. B. Verumi and D. S. Kadle, Enhanced and local heat transfer, pressure drop, and flow visualization for arrays of block-like electronic components, *Int. J. Heat Mass Transfer* **27,** 689–699 (1983).
6. E. M. Sparrow, A. A. Yanezmoreno and D. R. Otis, Convective heat transfer response to height differences in an array of block-like electronic equipments, *Int. J. Heat Mass Transfer* **28,** 469–473 (1984).
7. R. J. Moffat, A. Ortega and D. E. Arvizu, Cooling electronic components: forced convection experiments with an air-cooled array, *Heat Transfer in Electronic Equipment—1985*, ASME HTD-Vol. 48, pp. 15–27 (1985).
8. M. Faghri, R. C. Lessmann, S. Sridhar, R. Schmidt and Y. Asako, A preliminary experimental study of forced air-cooling of rectangular blocks encountered in electronic equipment, *ASME Winter Annual Meeting at San Francisco*, HTD-Vol. 123, pp. 1–6 (1989).
9. M. Faghri and Y. Asako, Turbulent three-dimensional heat transfer analysis of arrays of heated blocks, *9th International Heat Transfer Conference, Heat Transfer 1990*, Vol. 2, pp. 331–336 (1990).
10. S. V. Patankar, C. H. Liu and E. M. Sparrow, Fully developed flow and heat transfer in ducts having streamwise periodic variation of cross sectional area, *J. Heat Transfer* **99,** 180–186 (1977).
11. B. E. Launder and D. B. Spalding, The numerical computation of turbulent flows, *Comput. Methods Appl. Mech. Engng* **3,** 269–289 (1971).
12. S. V. Patankar, A calculation procedure for two-dimensional elliptic situations, *Numer. Heat Transfer* **4,** 409–425 (1981).

13. S. V. Patankar, *Numerical Heat Transfer and Fluid Flow*. Hemisphere, Washington D.C. (1980).
14. S. V. Patankar and C. Prakash, An analysis of the effect of plate thickness on laminar flow and heat transfer in interrupted-plate passages, *Int. J. Heat Mass Transfer* **24,** 1801–1810 (1981).
15. B. K. Lee, N. H. Cho and Y. D. Choi, Analysis of periodically fully developed turbulent flow and heat transfer by k–ε equation model in artificially roughened annulus, *Int. J. Heat Mass Transfer* **31,** 1797–1806 (1988).
16. R. W. Knight and M. E. Crawford, Numerical prediction of turbulent flow and heat transfer in channels with periodically varying cross sectional area, *ASME National Heat Transfer Conference at Houston*, HTD-Vol. 96, pp. 669–676 (1988).
17. G. S. Beavers, E. M. Sparrow and J. R. Lloyd, Low Reynolds number turbulent flow in large aspect ratio rectangular ducts, *J. Basic Engng* **93,** 296–299 (1971).
18. W. M. Kays and E. Y. Leung, Heat transfer in annular passages—hydrodynamically developed turbulent flow with arbitrarily prescribed heat flux, *Int. J. Heat Mass Transfer* **6,** 537–557 (1963).